TISSUE ENGINEERING: Part A
Volume 28, Numbers 9 and 10, 2022

DOI: 10.1089/ten.tea.2021.0078

termis
Tissue Engineering
& Regenerative Medicine
International Society

ORIGINAL ARTICLE

Targeted Activation of G-Protein Coupled Receptor-Mediated Ca^{2+} Signaling Drives Enhanced Cartilage-Like Matrix Formation

Ryan C. McDonough, PhD and Christopher Price, PhD

Intracellular calcium ($[Ca^{2+}]_i$) signaling is a critical regulator of chondrogenesis, chondrocyte differentiation, and cartilage development. Calcium (Ca^{2+}) signaling is known to direct processes that govern chondrocyte gene expression, protein synthesis, cytoskeletal remodeling, and cell fate. Control of chondrocyte/chondroprogenitor Ca^{2+} signaling has been attempted through mechanical and/or pharmacological activation of endogenous Ca^{2+} signaling transducers; however, such approaches can lack specificity and/or precision regarding Ca^{2+} activation mechanisms. Synthetic signaling platforms permitting precise and selective Ca^{2+} signal transduction can improve dissection of the roles that $[Ca^{2+}]_i$ signaling plays in chondrocyte behavior. One such platform is the chemogenetic DREADD (designer receptor exclusively activated by designer drugs) hM3Dq, which activates $[Ca^{2+}]_i$ signaling via the $G\alpha_q$-PLCβ-IP_3-ER pathway upon clozapine N-oxide (CNO) administration. We previously demonstrated hM3Dq's ability to precisely and synthetically initiate robust $[Ca^{2+}]_i$ transients and oscillatory $[Ca^{2+}]_i$ signaling in chondrocyte-like ATDC5 cells. Here, we investigate the effects that long-term CNO stimulatory culture have on hM3Dq $[Ca^{2+}]_i$ signaling dynamics, proliferation, and protein deposition in 2D ATDC5 cultures. Long-term culturing under repeated CNO stimulation modified the temporal dynamics of hM3Dq $[Ca^{2+}]_i$ signaling, increased cell proliferation, and enhanced matrix production in a CNO dose- and frequency-dependent manner, and triggered the formation of cell condensations that developed aligned, anisotropic neotissue structures rich in cartilaginous proteoglycans and collagens, all in the absence of differentiation inducers. This study demonstrated $G\alpha_q$-G-protein coupled receptor (GPCR)-mediated $[Ca^{2+}]_i$ signaling involvement in chondroprogenitor proliferation and cartilage-like matrix production, and it established hM3Dq as a powerful tool for elucidating the role of GPCR-mediated Ca^{2+} signaling in chondrogenesis and chondrocyte differentiation.

Keywords: chondrocyte calcium signaling, designer receptors exclusively activated by designer drugs, chemogenetics, G-protein coupled receptor activation, cartilage tissue engineering

Impact Statement

Targeted activation of intracellular calcium signaling has gained attention as a cartilage tissue engineering adjuvant approach. In the present study, we demonstrated that activation of hM3Dq, an engineered chemogenetic activator of the $G\alpha_q$-pathway and IP_3-mediated intracellular calcium signaling, drives accelerated development of mesenchyme-like cell condensations and cartilaginous neotissue formation in chondrocyte-like cell cultures *in vitro* and does so without the requirement of differentiation factors/inducers. These outcomes highlight the potential of targeted/synthetic $G\alpha_q$-pathway activation, specifically using novel chemogenetic approaches, to enhance the study of chondrocyte physiology and improve cartilage tissue engineering approaches.

Department of Biomedical Engineering, University of Delaware, Newark, Delaware, USA.

Introduction

Calcium (Ca^{2+}) is a requisite second messenger in chondrogenesis and chondrocyte differentiation, homoeostasis, and mechano-adaptation.[1,2] Several mechanically initiated (e.g., compression, shear, fluid flow, hydrostatic pressure, and osmotic load)[3–6] and ligand-driven (e.g., histamine, PTH, TGF-β)[7,8] intracellular calcium ($[Ca^{2+}]_i$) signaling pathways have been identified within chondrocytes, regulating Ca^{2+}-dependent chondrogenic processes through both ion channels, predominately associated with the transient receptor potential vanilloid 4 (TRPV4) ion channel, and G-protein coupled receptors (GPCRs).[9–12]

Despite being categorized as ''non-excitable'' cells, recent evidence indicates that precise modulation of chondrocyte $[Ca^{2+}]_i$ signaling is required for chondrogenesis,[13–15] differentiation,[16,17] and cell survival[18,19]; and for the anabolic and catabolic responses underpinning tissue development,[20] maturation,[2,21] and maintenance.[22] One critical aspect of this is oscillatory $[Ca^{2+}]_i$ signaling, where the presence, frequency, amplitude, and duration of $[Ca^{2+}]_i$ oscillations represent important determinants of chondrocyte, chondroprogenitor, and mesenchymal stem cell (MSC) behavior.[20,23]

Mature chondrocytes exhibit ''spontaneous'' long-period (>200 s) Ca^{2+} oscillatory behaviors,[24–26] and both primary and oscillatory $[Ca^{2+}]_i$ signaling behaviors can be enhanced by exposure to mechanical perturbations (and/or receptor ligands)[24,26,27]; indeed, exogenously driven Ca^{2+} oscillations mediate matrix anabolism in response to physiological loads.[28] Among chondroprogenitors, such as MSCs and chondroblasts, $[Ca^{2+}]_i$ oscillations support differential regulation of proteins and transcription factors encoding complex chondrogenic signaling behaviors.[29–32]

For example, during cartilage development, high-frequency $[Ca^{2+}]_i$ oscillations are associated with increased *SOX9* expression, cell proliferation, and matrix production[33–36]; whereas in MSCs, mechanical perturbations and receptor-mediated signaling drive chondrogenesis through $[Ca^{2+}]_i$ oscillation-dependent signaling pathways.[15,37,38] Importantly, oscillatory $[Ca^{2+}]_i$ signaling behaviors within chondrocytes rely on intracellular Ca^{2+} stores,[39,40] and they are modulated via a calcium signaling ''toolkit'' that sets up/sustains wave-like $[Ca^{2+}]_i$ feedback networks.[1,41–44]

Given the importance of well-regulated $[Ca^{2+}]_i$ signaling dynamics in chondrogenesis, chondrocyte differentiation, and cartilage development and homeostasis, a number of approaches have been explored to leverage exogenously tuned Ca^{2+} signaling to improve cartilage tissue engineering and regeneration.[2,7,21,45,46] For example, dynamic loading that drives elevated oscillatory Ca^{2+} signaling within chondrocyte-laden hydrogels enhances collagen and proteoglycan synthesis and matrix material properties.[28]

Similarly, driving Ca^{2+} oscillations in MSCs via electrical stimulation promotes chondrogenic outcomes in the absence of growth factors.[35,47] Several $[Ca^{2+}]_i$ regulating compounds (e.g., 4α-PDD, RN1734, and GSK1016790A) enhance pro-anabolic responses and cartilage tissue maturation *in vitro*[48]; driving oscillatory Ca^{2+} signaling in MSCs via GSK101, a TRPV4 agonist, enhances collagen deposition on patterned surfaces,[12] and gene, protein, and material property outcomes in ATDC5/chondrocyte-laden hydrogels.[45]

Although the field has leveraged endogenous control of native signaling pathways to interrogate $[Ca^{2+}]_i$ signaling influences on chondrogenesis, chondrocyte physiology, and cartilage development/tissue engineering/regeneration,[2,7,21,45] ''physiologically-mediated'' $[Ca^{2+}]_i$ manipulations are restricted to a rather small set of targets over which concerns exist regarding targeting specificity and precision. For example, mechanical stimulation can target numerous mechanosensitive components—some of which are not Ca^{2+} selective[49,50]—and can be damaging/injurious.

Alternatively, the use of biomolecules—either synthetic (e.g., GSK101) or natural (e.g., Histamine, PTH)—to target endogenous signaling pathways carries risks of off-target effects.[51,52] To overcome such limitations, we recently described a novel chemogenetic approach to drive highly specific and fully synthetic $[Ca^{2+}]_i$ signaling activation in a chondrocyte-like cell line.[40,53]

Designer receptors exclusively activated by designer drugs (DREADDs) represent a family of engineered chemogenetic GPCRs molecularly evolved to exhibit affinity to the pharmacologically inert compound, clozapine N-oxide (CNO), but not their native endogenous ligand, acetylcholine.[54] GPCRs, which signal through G-protein-linked (e.g., $G\alpha_s$, $G\alpha_{q/11}$, $G\alpha_i$, etc.) second messenger pathways, constitute the largest family of eukaryotic signal transducers and ~34% of clinical drug targets,[55–58] and both $G\alpha_{q/11}$- and $G\alpha_s$-dependent pathways have been implicated in chondrogenesis and chondrocyte physiology.[59]

$G\alpha_s$-, $G\alpha_i$-, and $G\alpha_q$-coupled DREADDs have been derived from mammalian muscarinic receptors.[60] rM3Ds (rat M3 muscarinic & turkey β1-adrenergic-derived $G\alpha_s$ GPCR) and hM4Di/KORD (human M4 muscarinic and human κ-opioid-derived $G\alpha_i$ GPCRs, respectively) indirectly modulate $[Ca^{2+}]_i$ signaling through the adenyl cyclase-cyclic AMP (cAMP) pathway.[61] hM3Dq (human M3 muscarinic $G\alpha_q$ GPCR) regulates $[Ca^{2+}]_i$ signaling directly through the ubiquitous $G\alpha_q$-PLCβ-IP_3 pathway and the release of Ca^{2+} from the endoplasmic reticulum (ER)[62], a pathway intimately associated with chondrocyte mechanotransduction[63] and oscillatory $[Ca^{2+}]_i$ signaling behaviors.[40,64]

Chemogenetics has transformed the study neural activity and behavior,[65,66] and it has seen application in some non-neuronal cell types (e.g., liver, kidney, pancreas)[67–69]; however, our work with hM3Dq represents the first application of chemogenetic approaches to study GPCR and downstream $[Ca^{2+}]_i$ signaling in musculoskeletal tissues.[40,53]

Using hM3Dq, we generated stably expressing mCherry-tagged hM3Dq-ATCD5 cells to study CNO-mediated Ca^{2+} signaling behaviors in chondrocyte-like cells.[40] We identified that CNO could drive, in a dose- and temperature-dependent manner, coordinated and widespread generation of a rapid primary $[Ca^{2+}]_i$ peak in hM3Dq ATDC5 cells, followed by sustained oscillatory Ca^{2+} signaling. Both primary and oscillatory $[Ca^{2+}]_i$ behaviors were cell-autonomous in nature, and they were reliant on internal ER Ca^{2+} stores and PLCβ-driven IP_3 dynamics, as opposed to store operated/external Ca^{2+} entry.[40]

In the present study, we investigated the role of hM3Dq-driven calcium signals on matrix synthesis in 2D ATDC5 cultures and relate how different levels of oscillatory signaling influence long-term cellular behaviors in response to repeated CNO stimulation. Incidentally, we demonstrated

that repeated stimulation of hM3Dq cells alters hM3Dq-mediated calcium signaling dynamics, does not negatively impact cellular health, and—in the absence of differentiation inducers—robustly drives cartilage-like neotissue formation and matrix deposition.

Overall, this work establishes the facile ability to synthetically drive $G\alpha_q$-dependent signaling cascades, ER-dependent Ca^{2+} release, and matrix deposition via hM3Dq in chondrocyte-like cells, providing a novel platform for studying GPCR and Ca^{2+} signaling responses within chondrocytes (and their precursors), and for testing chemogenetic means to enhance cartilage tissue engineering and regeneration.

Methods

Cell culture & experimental design

hM3Dq-mCherry-ATDC5 (hM3Dq) cells[40] were plated in tissue culture-treated well plates containing complete growth medium (CGM) [1:1 ratio Dulbecco's modified Eagle's medium and Ham's F12K (Caisson Labs), 5% fetal bovine serum (Sigma), 1×penicillin-streptomycin, and 10 μg/mL puromycin (ThermoFisher)] at 10,000 cells/cm^2 and cultured for 24 h. The samples were subject to stimulation with CNO (added for 30 min; Sigma), GSK1016790A (30 min; Tocris), or hypo-osmotic shock (30 s exposure). The CNO-stimulated samples received either 5, 50, or 500 nM CNO (1×, 10×and 100×the CNO EC_{50} previously identified[40]) in HBSS 1×/week, 1×/day, or 3×/day for 2 weeks.

GSK101 (10 nM in HBSS) and hypo-osmotic shock (CGM diluted 50% with diH2O) groups were stimulated 1×/day. After stimulation, old media were aspirated and fresh CGM added. Unstimulated hM3Dq cells, and wild-type cells (WT) receiving 1×/day 500 nM CNO or no CNO, served as negative controls. All samples were incubated and tested at 37°C, 5% CO_2; media were changed every other day for samples not stimulated daily. All matrix and health assessments were performed in biological and technical triplicate ($n = 3 \times 3$/group); all calcium imaging assays were performed in technical triplicate ($n = 3$/group).

Calcium imaging

Cells plated in 12-well glass-bottom plates (TissueTek) and treated once daily with 500 nM CNO, a concentration established based on CNO levels eliciting maximum oscillatory $[Ca^{2+}]_i$ signaling behaviors,[40] were subject to calcium imaging after 1, 3, 7, and 14 days of stimulatory culture. Cells were stained with 5 μM Fluo-8AM, washed in HBSS, and their CNO-evoked $[Ca^{2+}]_i$ signaling response imaged as previously described.[40]

Briefly, each sample was imaged for 15 min on a Zeiss AxioObserver.Z1 Apotome.2 under temperature control (37°C), with the first 5 min of the imaging period used to establish baseline Ca^{2+} signaling behaviors and the subsequent 10 min the CNO-mediated Ca^{2+} response. All studies were performed in Ca^{2+} replete media. A custom MATLAB program[40,53] was used to isolate the $[Ca^{2+}]_i$ signals of individual cells in each image series.

Within these traces, we defined a calcium peak as an increase in Fluo-8AM intensity larger than three standard deviations from the baseline (average of first 5-min) fluorescence. Ca^{2+} signaling parameters assessed in this study included: the percent of cells exhibiting a primary $[Ca^{2+}]_i$ peak, and 2+, 5+, and 9+ peaks after CNO administration/stimulation; the number of peaks elicited; the amplitude (i.e., height) and duration of each peak; and the period between adjacent peaks (peak-to-peak period).

Cell health assays

Location-referenced differential interference contrast imaging was used to longitudinally track cell proliferation in hM3Dq cultures. Cell health was assessed at 1-, 3-, and 14 days via Live/Dead staining (viability), where cells were incubated in 2 μM Calcein AM (''live'' cell indicator) and 4 μM ethidium homodimer-1 (''dead'' cell indicator; ThermoFisher) for 30 min; or via apoptosis staining, where cells were incubated in 5 μM CellEvent Caspase 3/7 Detection Reagent (apoptosis indicator; ThermoFisher) and 1 μM Hoechst 33342 (nuclear stain; ThermoFisher) for 30 min.

Histology & immunocytochemistry

Micro-mass cultures were fixed in 4% paraformaldehyde at day 7 and 14, and were stained with Picrosirius Red (StatLab), or Alizarin Red (2% Alizarin Red S (Sigma), pH 4.2) and Alcian Blue (1% Alcian Blue 8GX (Sigma) +3% glacial acetic acid, pH 2.5).[70] Separately, immunocytochemistry (ICC) samples were fixed, blocked, permeabilized (0.2% Triton-X + 2% BSA in PBS), and incubated with rabbit anti-collagen type 1 (Polyclonal; 2 μg/mL; PA1-85319), mouse anti-collagen type 2 (Monoclonal; 2 μg/mL; MA5-12789), or rabbit anti-aggrecan (Polyclonal; 1:500 dilution; 13880-1-AP) antibodies (ThermoFisher); then, they were detected with appropriate Alexa Fluor 488-conjugated secondary antibodies (1:500 dilution; ThermoFisher).

Tiled images of histological and ICC samples were captured at 5×magnification across each well, with higher magnification images captured for cell morphology and nodule structure assessment.

Image & statistical analysis

Custom image analysis macros were developed in Fiji (ImageJ) to quantify (i) geometrical and spatial properties and (ii) collagen deposition/staining within cartilage-like cell condensations during 2D hM3Dq cell culture and CNO stimulation (Supplementary Fig. S1). Nodule area, area fraction, Feret's diameter, aspect ratio, nodule density, and distance between adjacent nodules are reported. Picrosirius red staining of collagen-rich matrix deposition was assessed via hue, saturation, and value (HSV) analysis of stain color, brilliance/vibrancy, and darkness/shade, respectively.

Statistical analysis was performed in Prism v8 (GraphPad Software; La Jolla, CA). Data outliers were identified using the ROUT method.[71] *t*-tests, one-way ANOVAs (single CNO stimulation), two-way ANOVAs (repeated CNO stimulation), and their non-parametric equivalents, with *post hoc* testing, as well as regression analysis were performed where appropriate. All data are presented as mean ± range. The threshold for statistical significance was set at a multiplicity correct *p*-value of $p < 0.05$.

Experiment

CNO-evoked $[Ca^{2+}]_i$ signaling in hM3Dq cells during long-term, daily stimulatory culture

hM3Dq-ATDC5 cells robustly responded to CNO over the entire 14-day culture; however, the temporal dynamics of CNO-mediated $[Ca^{2+}]_i$ responses changed over time. Among hM3Dq cultures stimulated 1×/daily (500 nM), >80% of cells exhibited CNO-evoked $[Ca^{2+}]_i$ signaling (Fig. 1A). A maximum of ~82% of hM3Dq cells exhibited two-plus Ca^{2+} peaks in response to CNO (at day 7), whereas values at day 1 and 14 were similar.

As early as day 3, reduced CNO-evoked Ca^{2+} oscillation capacity was seen, and only ~4% of cells elicited 9+ peaks (down from ~14%), further dropping to ~1% at day 14. The average number of $[Ca^{2+}]_i$ peaks elicited by CNO, across our 10-min post-CNO imaging window, decreased from 4.23 peaks/cell at day 1 to 2.15 peaks/cell at day 14 (Fig. 1B). Regarding the temporal dynamics of $[Ca^{2+}]_i$ signals, both CNO-induced primary and oscillatory Ca^{2+} peak amplitudes were highest at day 1 of culture (33 and 15–5 a.u., respectively).

Under continued stimulatory culture, primary $[Ca^{2+}]_i$ peak heights decreased (13–18 a.u.; $p < 0.05$), whereas secondary peak amplitudes approached a plateau of ~2–3 a.u. (Fig. 2A). The interval between the first two CNO-evoked Ca^{2+} peaks (i.e., peak interval 1) decreased with stimulatory culture, from ~155 s to ~106 s; however, subsequent changes in peak-to-peak periods were largely consistent among groups (Fig. 2B). $[Ca^{2+}]_i$ oscillation peak intensity decreased from ~11 to ~5 a.u. by day 3 of stimulatory culture, whereas oscillation periods decreased more gradually, from ~116 s at day 1 to ~85 s at day 14. (Fig. 2C, D, respectively).

The duration of the first calcium peak elicited by CNO, as well as those of secondary Ca^{2+} peaks appeared minimally influenced by stimulatory culture, dropping from 79 s to 59 s, and from 41 s to 30 s, respectively, over the 14-day culture (Supplementary Fig. S2).

Frequent activation of hM3Dq-mediated $[Ca^{2+}]_i$ signaling does not negatively impact cell health

Treatment of hM3Dq cells with CNO resulted in qualitative concentration- and dosing frequency-dependent increases in cell proliferation (Fig. 3A). Assessment of hM3Dq cell viability indicated >95% viability after 24- and 72 h of CNO stimulation (all groups); unstimulated WT cells experienced an insignificant reduction in viability at 72 h (Fig. 3B). Conversely, hM3Dq cells receiving once- and thrice-daily CNO stimulation had significantly increased viability at 72 h compared with 24 h.

No significant changes in viability were observed between CNO-stimulated and GSK101/Hypo-osmotic shock-stimulated groups; however, a significant difference in WT viability at 72 h compared with the daily stimulated samples was seen (5.1% ± 2.4% for WT vs. >98% ± 0.2–0.5% for 1×/day & 3×/day CNO, GSK101, Hypo). Caspase activity assessment found <4% of cells positive for apoptosis after 24- or 72°h of treatment.

Although nearly all groups exhibited increases in apoptosis between 24 and 72 h, statistically significant changes were only seen in the single CNO treated, 1×/day 500 nM CNO, 3×/day 50 nM CNO, and 1×/day GSK101 groups ($p < 0.05$; Fig. 3C). Among the 1× and 3× daily stimulated groups, consistently lower levels of apoptosis (<2% of hM3Dq cells) were observed at 72 h compared with control cultures (Fig. 3C). In a group of hM3Dq cultures stimulated 1×/daily with 500 nM CNO for 2 weeks, >92% cell viability and <5% apoptosis was observed (Fig. 3D).

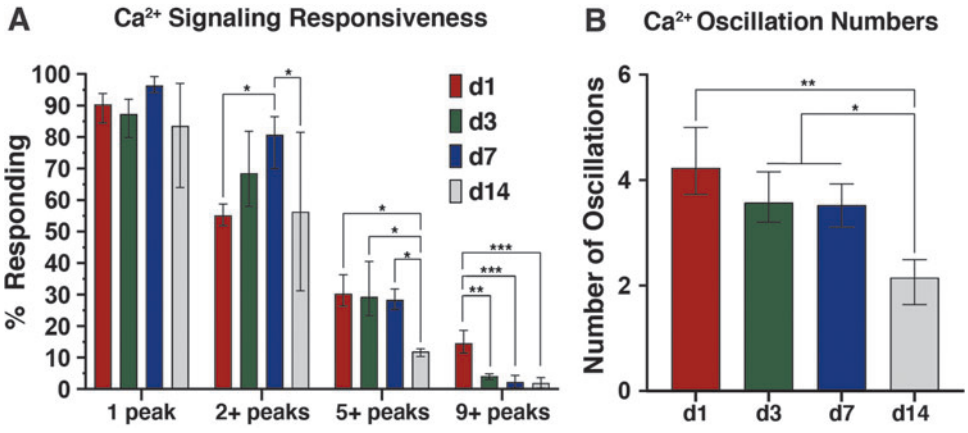

FIG. 1. Primary and oscillatory calcium signaling responses of hM3Dq-ATDC5 cells subjected to once-daily 500 nM CNO administration during long-term stimulatory culture. **(A)** CNO-evoked primary Ca^{2+} responses remained largely unchanged across 14 days of daily stimulatory culture; however, oscillatory Ca^{2+} signaling behaviors changed over time. The number of cells exhibiting 2+ peaks significantly increased through day 7 of culture (compared with days 1 and 14), whereas extensive oscillatory behaviors significantly diminished at day 14; the number of cells exhibiting 5+ peaks remained stable through day 7 (at ~28–30%), then dropped to ~11% at day 14; and the number of cells exhibiting 9+ peaks was suppressed from day 3 onward, dropping from ~14% to <5%. **(B)** The average number of oscillations per cell gradually diminished through day 7 of culture, dropping from 4.2 peaks/cell to ~3.5 peaks, then to ~2.2 peaks/cell at day 14. *$p < 0.05$, **$p < 0.01$, ***$p < 0.001$; one-way ANOVA with Tukey's *post hoc* test. CNO, clozapine N-oxide.

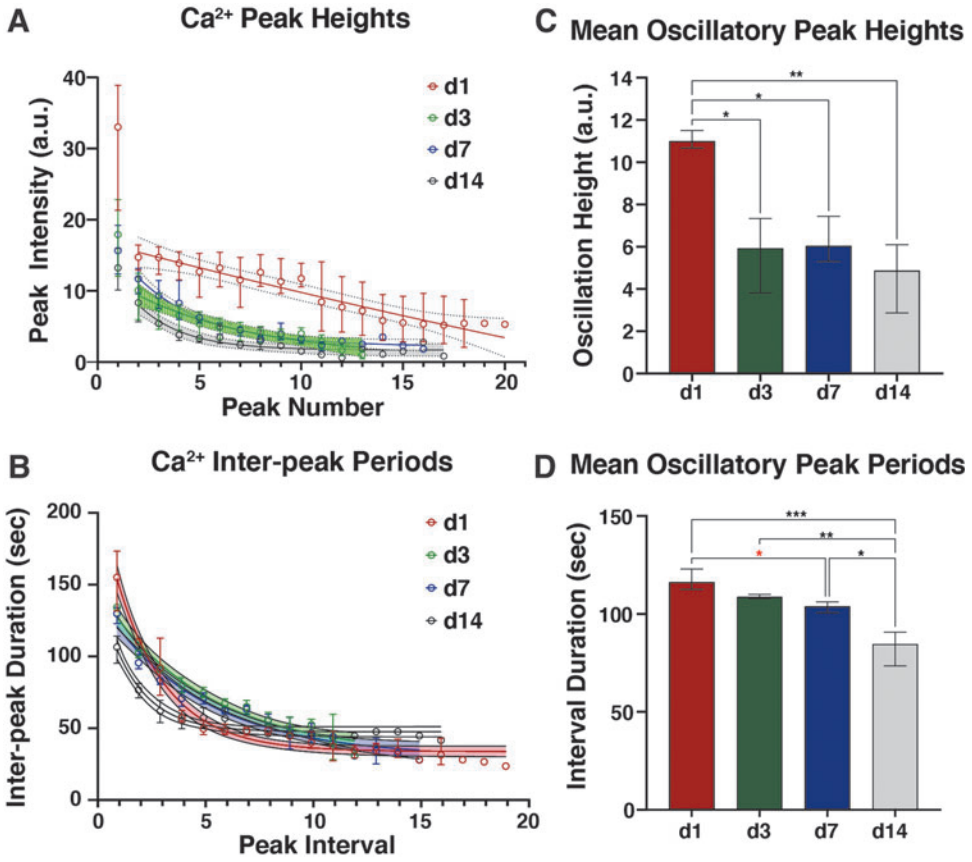

FIG. 2. Temporal dynamics of CNO-induced Ca^{2+} oscillations in hM3Dq-ATDC5 cells during long-term stimulatory culture. **(A)** Stimulation with 500 nM CNO at day 1 of culture elicited mean primary Ca^{2+} peak intensities of ~33 a.u., which quickly dropped to ~15 a.u. at the second peak and decayed linearly to ~5 a.u. for later peaks. At day 3 of culture and beyond, significantly reduced primary peak intensities (~13–18 a.u.; $p < 0.05$, one-way ANOVA with Tukey's *post hoc* test), which decayed to 2–3 a.u. at later peaks, were observed. **(B)** Peak-to-peak periods exhibited similar dynamics across all culture timepoints; the first peak interval (i.e., between the primary and initial secondary peak) was always longer than all subsequent intervals, which decayed to a plateau between 25 and 45 s. The initial inter-peak period decreased—non-significantly—from ~160 s at day 1 to ~130–135 s at days 3 and 7, and significantly to ~105 s at day 14 ($p < 0.01$, one-way ANOVA with Tukey's *post hoc* test). **(C)** Mean Ca^{2+} oscillation height decreased significantly from ~11 a.u. at day 1 to ~5 a.u. at day 3 and beyond. **(D)** Mean oscillation peak-to-peak period gradually decreased from ~116 s at day 1 to ~108 s at day 3, then to ~105 s at day 7 and ~85 s at day 14. *$p < 0.05$, **$p < 0.01$, ***$p < 0.001$; one-way ANOVA with Tukey's *post hoc* test. The statistical comparisons indicated in red fell just short of significance, $p < 0.10$.

CNO-driven, hM3Dq-mediated $[Ca^{2+}]_i$ signaling enhances matrix deposition

Stimulating hM3Dq cells with CNO drove concentration- and dosing frequency-dependent increases in matrix deposition over 14 days of culture; cultures stimulated daily with CNO formed layered, tissue-like cartilaginous nodules rich in proteoglycan (Alcian Blue) and collagen content (Picrosirius Red) (Fig. 4 and Supplementary Fig. S3). Nodules, or ''neotissue'' condensations, were rarely seen in unstimulated, daily hypo-osmotic shock, and daily GSK101-treated cultures. Under reduced stimulatory pressure (e.g., lower CNO concentration and/or reduced frequency), smaller, more rounded nodules with greater cellular homogeneity and reduced matrix staining were observed.

With increasing stimulation frequency and CNO concentration nodule size increased, tissue and cellular heterogeneity increased, and deeper staining for cartilage matrix proteins, and increasing cell/tissue organization and alignment were observed (Supplementary Fig. S4). Morphologically, these nodules exhibited a dense, layered, central cellular mass with richly stained proteoglycan and collagen extracellular matrix (ECM), and often, ''arms'' of highly aligned neotissue protruding from the central masses toward and connecting to adjacent nodules.

Higher-resolution images revealed much diversity in nodule cell morphology, especially compared with the ''cobblestone''-shaped appearance of ATDC5 cells in monolayer regions between nodules (Supplementary Fig. S5). At nodule edges/peripheries, and within regions of neotissue exhibiting cellular alignment, cells exhibited ''spindle-like'' appearances. Moving toward the nodule centers, cells having a more rounded morphology were observed, with ''hypertrophic'' appearing cells regularly seen by 14 days of stimulatory culture.

Quantitatively, average nodule area, area fraction, and nodule length (i.e., Feret's diameter) increased dramatically with CNO dosing frequency and concentration (Fig. 5A–C). Interestingly, although area-corrected nodule density (i.e., nodule number/well area) increased after CNO administration, it did

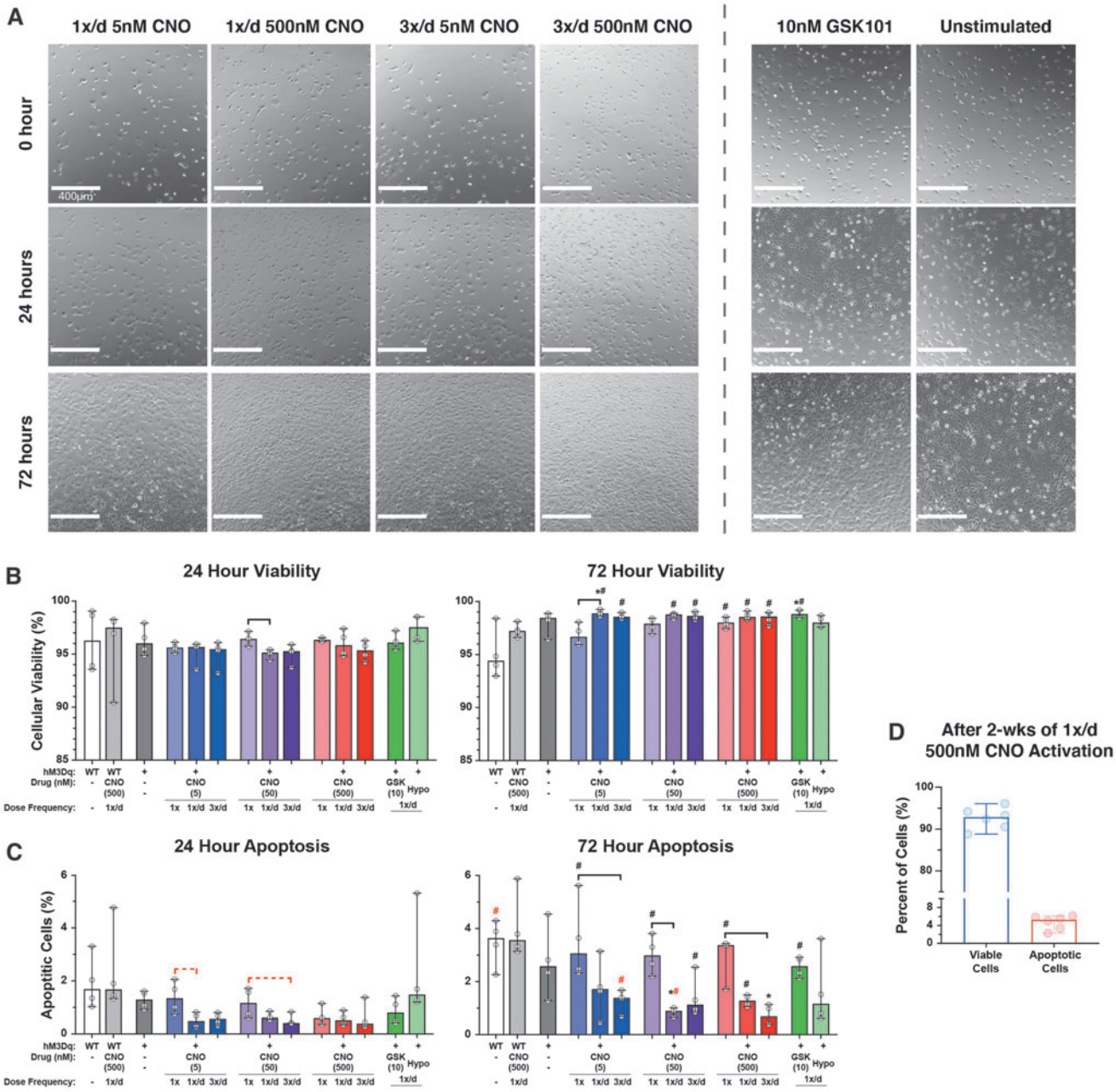

FIG. 3. Effect of CNO stimulation on hM3Dq cell proliferation and health during early stimulatory culture. **(A)** Location-matched DIC images revealed CNO concentration and frequency-dependent increases in the proliferative capacity of hM3Dq cells; elevated stimulatory pressures induced increased cell proliferation compared with less-frequent and lower concentration stimulation; however, all CNO stimulated groups appeared to proliferate faster than the non-CNO groups. **(B)** Cell viability was quite consistent among all groups after 24 h of culture, at >95% cells. At 72 h, only unstimulated WT cells experienced a—minor—decrease in viability, dropping from 96% to 94%; no significant changes in viability were observed among WT or unstimulated hM3Dq cells; and hM3Dq cells multiply stimulated with CNO or GSK101 saw significant increases in viability at 72 h compared with 24 h, increasing by $\sim$2–3% percentage points. **(C)** Apoptosis for all groups increased at 72 h compared with 24 h, but this increase was significantly suppressed in multiply stimulated hM3Dq cells in a concentration- and frequency-dependent manner; the highest CNO-stimulated group (3×/day 500 nM) displayed <1% apoptosis. **(D)** Viability and apoptosis in hM3Dq cells stimulated once daily with 500 nM CNO was very high (>92%) and low (<5%), respectively, after 2 weeks of culture. $^{*}p<0.05$ compared with WT (& WT+CNO), Kruskal–Wallis test with Dunn's multiple-corrections tests. Bar $=p<0.05$ for the comparison between indicated groups for the noted CNO concentration, Kruskal–Wallis test with Dunn's multiple-correction tests. $^{\#}p<0.05$ for comparison between respective 72- and 24-h outcomes, Mann–Whitney test. Statistical comparisons indicated in red are those that fell just short of significance, $p=0.0558$ for Kruskal–Wallis test and $p=0.0571$ for Mann–Whitney test. DIC, differential interference contrast.

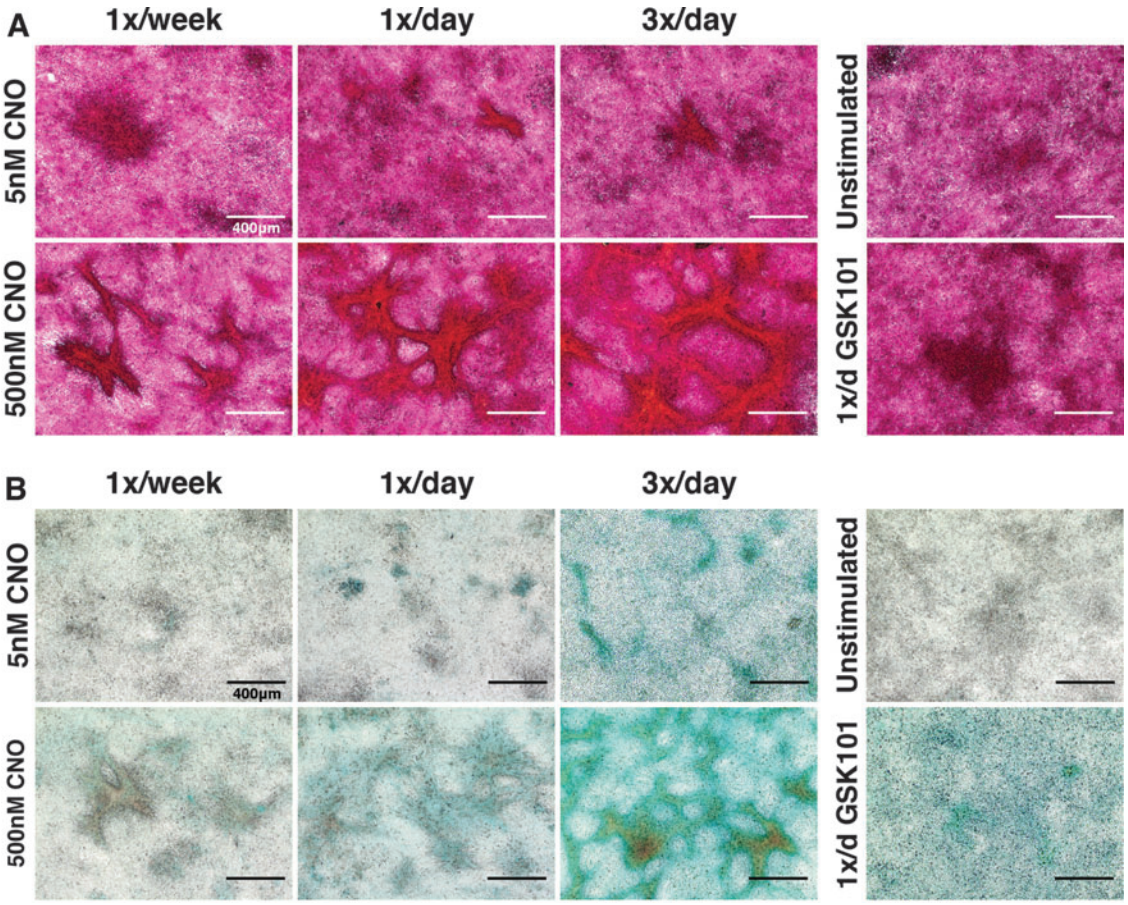

FIG. 4. CNO stimulation of hM3Dq-ATDC5 cells drove concentration- and frequency-dependent neotissue formation. **(A)** PR staining demonstrated deep and robust staining for collagens within cell condensations/nodules formed following 2 weeks of CNO stimulatory culture. The size and alignment of tissue nodules increased with CNO concentration and dosing frequency; PR staining of nodules changed from a *purple/deep red* under lower CNO stimulation regimes to *bright red-orange* with increased stimulation pressure (reflecting increased collagen content), whereas inter-territorial cells stained *light pink/light purple* (indicating little to no collagen deposition). *Purple/deep red* stained cell clumps were observed in GSK101-treated and unstimulated micromass cultures; however, these cells did not exhibit the tissue alignment and condensations observed in the CNO-treated cultures. **(B)** Similar outcomes were observed for AB staining of proteoglycans; CNO induced concentration- and frequency-dependent enhancements in proteoglycan deposition (*blue*). GSK101-stimulated cultures developed appreciable AB staining, though this was more diffuse compared with CNO cultures, whereas unstimulated cultures were relatively devoid of AB staining. AB, alcian blue; PR, picrosirius red.

FIG. 5. Analysis of neotissue nodule geometries and shape descriptors and collagen staining intensity after long-term stimulatory culture (14 days). **(A)** Average nodule size increased in a CNO dose- and frequency-dependent manner, from $\sim 20{,}000\,\mu m^2$ in the least stimulated group to $\sim 120{,}000\,\mu m^2$ and $\sim 320{,}000\,\mu m^2$ in the thrice-daily 50 and 500 nM CNO-stimulated groups, respectively ($p < 0.001$). GSK101 and hypo-osmotic shock (HS) areas were indistinguishable from those of WT and unstimulated hM3Dq cultures. *Circles* having sizes scaled to total nodule areas are provided above the figure for visual reference. **(B)** The area fraction of nodules increased with CNO concentration and frequency; from $\sim$4–7% in the $1\times$/week groups to $\sim$10% in the 5 nM CNO group and $\sim$24–38% in the 50 and 500 nM groups, respectively, when stimulated with CNO thrice daily ($p < 0.001$). Area fractions for GSK101 and HS-stimulated cultures were indistinguishable from those of WT/unstimulated cultures. **(C)** Similar CNO dose and frequency-dependent increases in the Feret's diameter of formed nodules (i.e., maximal geometric width) were observed. *Circles* having diameters and aspect ratios scaled to demonstrate treatment-dependent changes in nodule size and shapes are provided above the figure for visual reference. **(D)** Analyzing the aspect ratio of formed neotissue nodules demonstrated increasing elongation with increasing CNO dose and stimulation frequency. **(E)** Changes in collagen staining, that is, PR stain color, brilliance (*gray* content), and intensity, were assayed via measures of hue, saturation, and value, respectively. With increasing CNO concentration and dose-frequency, the stained collagen-rich tissues exhibited *deeper* ($\sim$0.7–0.8) and *darker* ($\sim$0.2–0.4) *blue-red* ($\sim 350°$) colors, indicative of increased collagen deposition. In **(E)**, as well as **(A, C)**, the colors of the indicated *circles* have been matched to the average HSV values of the group. $^*p < 0.05$ compared with WT (& WT+CNO), bar $= p < 0.05$ for the comparison between indicated groups for the noted CNO concentration, $^1p < 0.05$ compared with once-only activation at the noted CNO concentration, and $^5p < 0.05$ compared with the 5 nM CNO activation for the same administration frequency; Kruskal–Wallis test with Dunn's multiple-correction tests. Statistical comparisons indicated in red are those that fell just short of significance, $p < 0.1$.

not differ markedly among CNO-treatment conditions (Supplementary Fig. S6). We also observed that nodules typically displayed anisotropic morphologies (aspect ratio >2), ''elongating'' markedly with CNO dosing frequency and concentration ($p < 0.05$) compared to hypo-osmotic shock, GSK101, and unstimulated cultures ($p < 0.001$) (Fig. 5D).

In quantifying Picrosirius red-stained neotissue cultures, via hue, saturation, and value (HSV) assessment, we observed clear influences of CNO concentration, frequency-of-dosing, and time-in-stimulatory-culture on collagen-rich matrix deposition (Fig. 5E). When assessed using a $\sim 31\,mm^2$ region of interest ($\sim 10\%$ of the culture well

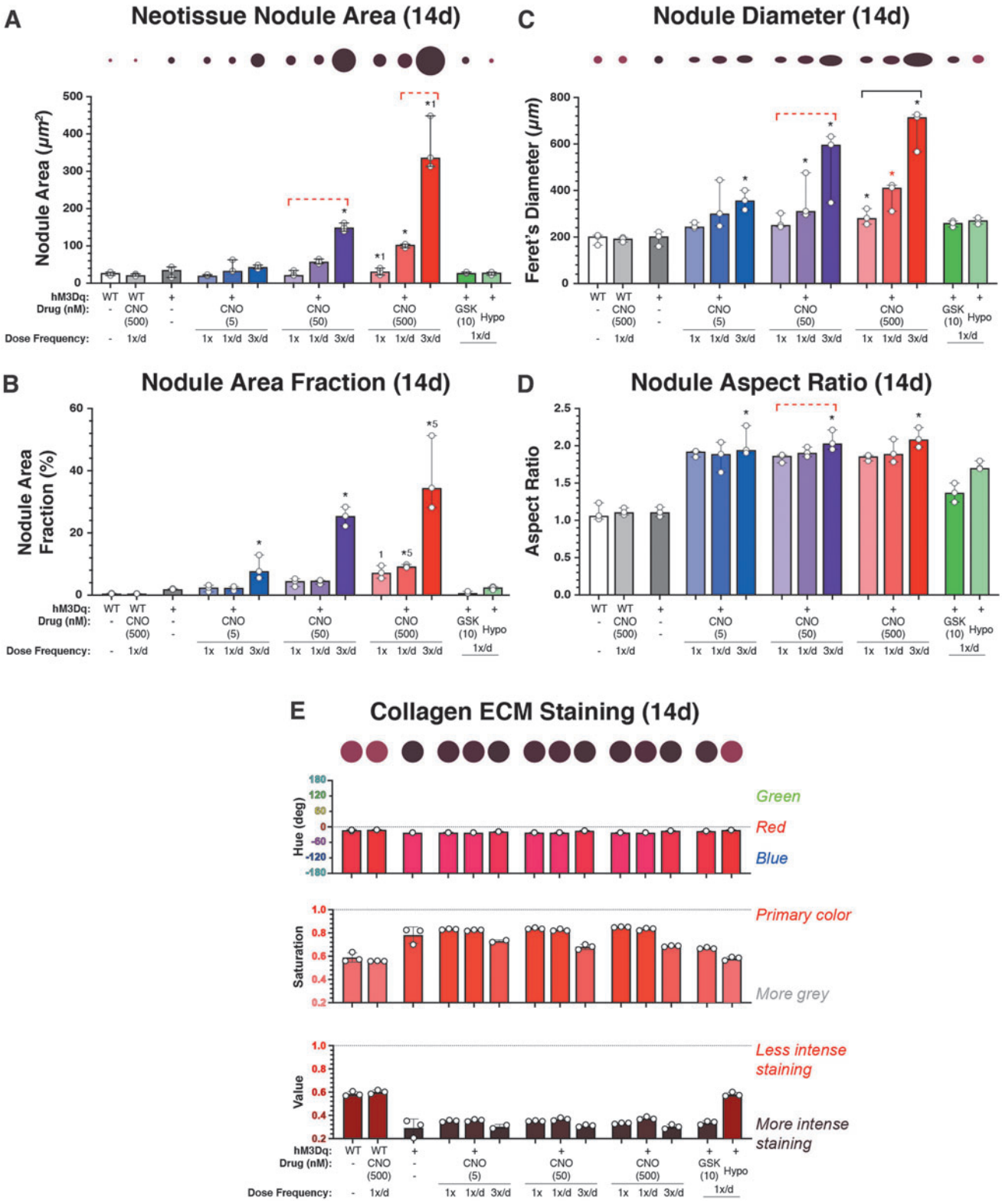

area), we observed that all cultures exhibited some degree of collagen-rich tissue deposition.

Staining at 14 days was always more intense than at 7 days (not shown). At the 14-day timepoint, all cultures exhibited the expected blue–red to red Picrosirius red (*hue* = 340 to 356°) staining, indicating the deposition of collagen-rich matrix. However, CNO-stimulated hM3Dq-ATDC5 tissues were more vibrant (*saturation* = 0.68–0.85) and stained more intensely/darker (*value* = 0.38–0.30) than unstimulated cultures (*saturation* = ~0.58 and value = ~0.59).

Collagen staining intensity also appeared to increase with CNO concentration and dose-frequency, which is conveyed qualitatively in the representative Picrosirius red-stained palettes depicted in Figure 5E. GSK101 and hypo-osmotically loaded cultures exhibited collagen staining behaviors that fell between the CNO-treated and -untreated cultures. Lastly, ICC staining of ECM deposition revealed the matrix composition in CNO-stimulated hM3Dq cultures to favor collagen type II and aggrecan, with an appreciable but less extensive presence of collagen type I (Fig. 6 and Supplementary Fig. S7).

Discussion

Directed activation of $[Ca^{2+}]_i$ signaling and calcium-dependent processes has emerged as a promising approach to exogenously drive the chondrogenic and anabolic pathways required for successful cartilage tissue engineering and regeneration.[2,28,35,45] Extensive research on $[Ca^{2+}]_i$ signaling in chondrocytes has revealed numerous pathways/approaches by which Ca^{2+} activation and Ca^{2+}-dependent processes can be controlled in chondrocytes, establishing a critical role for $[Ca^{2+}]_i$ signaling dynamics in chondrocyte and cartilage development/physiology.[2,15,22,72–74]

However, although native Ca^{2+} signal transducers can be used to direct chondrogenic responses, they have limited ability to precisely dissect Ca^{2+}-specific processes from those of divergent/convergent signaling pathways, or to control individual cell behavior within mixed cells populations and tissues.[49–52] In contrast, controlling $[Ca^{2+}]_i$ signaling by synthetic means, such as through chemogenetic DREADDs, offers a more precise, one-to-one stimulation paradigm for dissecting the influence of Ca^{2+} signaling behaviors on chondrocyte physiology, and cartilage development and homeostasis, disease etiology, and tissue engineering/regeneration.

Using ATDC5 cells engineered to stably express the synthetic DREADD hM3Dq[60]—which drives PLCβ-IP_3-mediated Ca^{2+} release from internal stores (the ER) in an oscillatory manner upon CNO administration—we demonstrated that chemogenetic activation of $G\alpha_q$-signaling promotes cartilage-like neotissue formation. ATDC5 cells are a well-established model for studying chondrogenesis,[75–78]

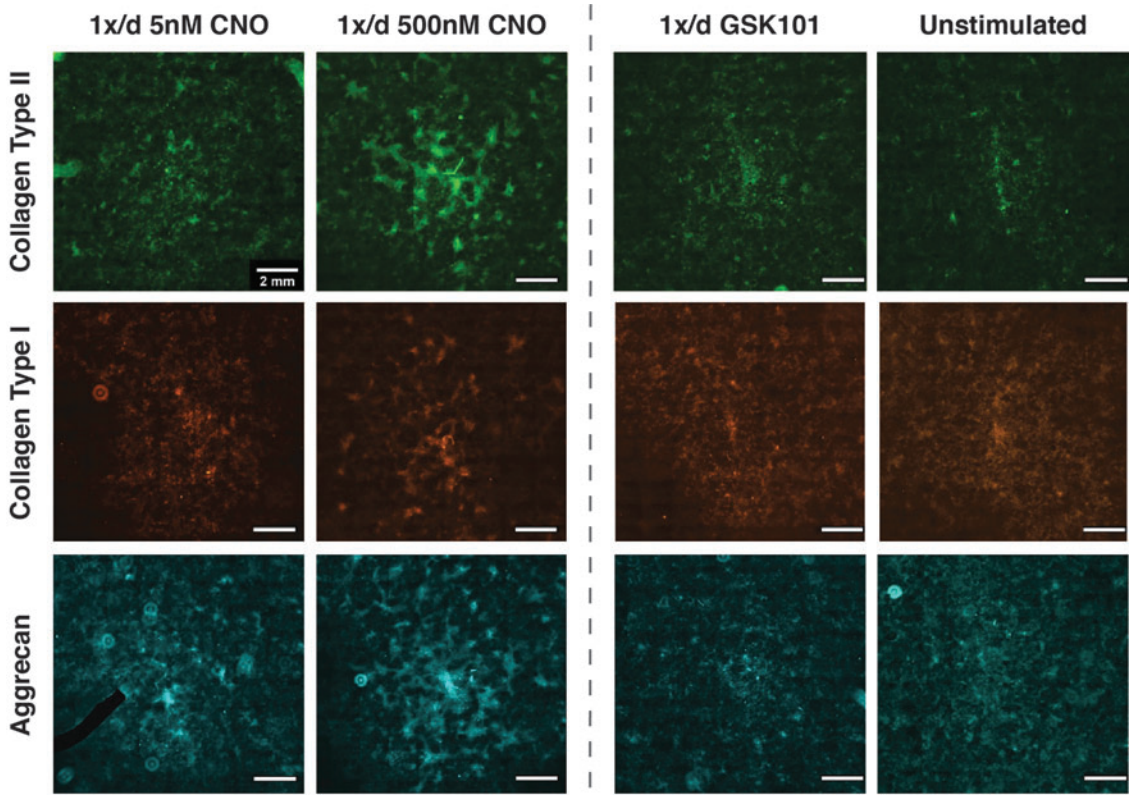

FIG. 6. ICC staining revealed that CNO-mediated activation of hM3Dq enhanced collagen type II and aggrecan deposition. CNO stimulation resulted in the qualitative appearance of concentration-dependent enhancement of antibody staining for collagen type II (*top row*) and aggrecan (*bottom row*). Once-daily stimulation with 500 nM CNO exhibited the highest levels of deposition of both proteins, whereas 5 nM CNO displayed increased staining relative to GSK101 and unstimulated cultures; appreciable but reduced staining for collagen type I (*middle row*) was also detected. The *black region* in the 1×/day 5 nM CNO aggrecan image is a ''masked-out'' fluorescent dust particle.

however, the chondrogenic transformation of ATDC5 cells (and de-differentiated chondrocytes) requires extended culture in the presence of specific differentiation inducers.[75,76,78]

This distinction is critical, as the present study was conducted in the absence of differentiation adjuvants; these outcomes speak to the influence of $G\alpha_q$-mediated signal transduction and $[Ca^{2+}]_i$ signaling on chondroprogenitor behaviors, as well as their role in directly regulating chondrogenesis, tissue formation, and matrix synthesis.

In hM3Dq-ATDC5 cultures, hM3Dq-mediated primary $[Ca^{2+}]_i$ signal generation was stable across 14 days of stimulatory culture (1×/day at 500 nM CNO). Extensive oscillatory signaling behaviors (9+ peaks) decreased from 3 days onward, whereas robust 5+ and 2+ peak responsiveness and oscillatory behaviors were retained through 1 week of culture. In contrast, the temporal dynamics of CNO-evoked $[Ca^{2+}]_i$ signaling changed abruptly under daily CNO activation, with the largest CNO-evoked primary and oscillatory Ca^{2+} intensities recorded on day one of stimulatory culture and then consistently reduced across longer culture periods.

Changes in Ca^{2+} signaling dynamics accompany contact inhibition, cytoskeletal remodeling, and upregulation of calcium buffering proteins, such as calmodulin, which occur as cells proliferate and/or adapt to their Ca^{2+} signaling ''environment''.[79–85] Given the proliferation and tissue/nodule formation seen with daily CNO stimulation, changes in hM3Dq-mediated $[Ca^{2+}]_i$ signaling behaviors were not entirely unexpected. Indeed, fibroblast-like cells exhibit faster oscillatory signaling with increasing cell density and substrate stiffness.[86,87] Alternatively, MSC maturation is accompanied by reduced Ca^{2+} oscillations as they differentiate and lay down ECM, exhibiting only infrequent, spontaneous ''oscillations'' unless perturbed.[88]

In addition, pharmacological stimulation of PKC, immediately downstream of $G\alpha_q$, promotes chondrocyte differentiation.[41,89] Therefore, reductions in CNO-mediated oscillatory signaling behaviors with extended stimulatory culture may be explained by hM3Dq-driven neotissue formation and matrix deposition.

In 2D culture, ATDC5 cells rapidly proliferate to form confluent monolayers before becoming contact inhibited, similar to what is seen in limb bud rudiments *in vivo*.[75,76] The first difference we noticed among CNO and control hM3Dq cultures was a concentration and dosing frequency-dependent increase in cell proliferation. It is noted that $G\alpha_q$ activation regulates cell cycle progression and proliferation across numerous cells; in chondrocytes, $G\alpha_q$-GPCR signaling is involved in mitigating apoptotic signaling[53,90] and is necessary for stem cell-like chondrocyte survival in the growth plate.[59,90]

Activation of $[Ca^{2+}]_i$, however, represents a double-edged sword. While $[Ca^{2+}]_i$ signaling is a requisite for numerous chondrocyte processes, excessive calcium signaling can be detrimental, triggering apoptosis, non-chondrogenic responses, and disease.[18,90–94] Investigating the effects of different hM3Dq activation regimes—including 3 days of thrice daily administration of CNO at ~100 times its EC50 dose—on ATDC5 health demonstrated minimal impact on cell viability or apoptosis.

Further, the health of cultures treated once daily with 500 nM CNO for 2 weeks appeared unaffected, even following neotissue development. These outcomes confirm that the hM3Dq signaling platform can safely and repeatedly invoke $G\alpha_q$-GPCR-mediated $[Ca^{2+}]_i$ signaling.[53] We also note that this platform offers additional safety compared with ion channel targeting approaches, as activated $G\alpha_q$-GPCRs are rapidly internalized, via endocytosis, for degradation or recycling, to limit constitutive $G\alpha_q$-coupled receptor activation and elevated $[Ca^{2+}]_i$ levels.[95,96]

Following hM3Dq-mediated increases in ATDC5 proliferation, synthetic $G\alpha_q$ activation fostered drastic changes in chondrogenic ATDC5 cell behavior. Activation of hM3Dq drove the formation of ''tissue nodules'' that exhibited complex cellular morphologies/phenotypes, aligned ''tissue'' structures, and robust collagen- and proteoglycan-rich cartilaginous ECM deposition. As little as two, once-weekly CNO administrations had an observable influence on nodule formation; at 5 nM, weekly CNO administration resulted in the appearance of ''round'' regions of increased cell density (i.e., condensations) with modest matrix staining, similar to those of daily 10 nM GSK101 activation.

Weekly 500 nM CNO generated more complex neotissues, with evidence of heterogenous cell populations, aligned structures, and deep collagen and proteoglycan staining. When exposed to higher CNO concentrations and/or frequencies of administration, developing hM3Dq neotissues displayed cell morphologies reminiscent of various stages of chondrogenesis and differentiation. Surrounding each nodule, a monolayer of ''quiescent,'' contact-inhibited cells having ''fibroblastic'' appearance were observed, consistent with the undifferentiated ATDC5 phenotype.[75,76]

In nascent condensations and at nodule edges, ''spindle-like'' cells were found. Within nodule centers, smaller cells having round morphology were present; at later time points, these appeared to transition into enlarged cells of ''hypertrophic'' appearance. Analysis of Picrosirius red-stained cultures revealed CNO concentration-, CNO dosing frequency-, and time in stimulatory culture-dependent increases in matrix deposition/maturation.

Subsequently, ICC staining demonstrated that the matrix synthesized in stimulated hM3Dq cultures was collagen type II and aggrecan rich, with collagen type I present to a lesser degree. The morphology of the nodules in highly simulated cultures was noteworthy, having complex, non-ellipsoidal, and anisotropic structures, which appeared to form bridged ''networks'' of interconnected neotissues under greater CNO stimulation.

Overall, the nodules and neotissues formed by synthetically driving $G\alpha_q$- (and $[Ca^{2+}]_i$) signaling in hM3Dq cells remind one of those observed in early limb development, where MSCs coalesce into mesenchymal condensations, differentiate into chondrocytes that deposit a proteoglycan- and collage type II-rich ECM, and then undergo hypertrophy.[97–102] Although such endochondral ossification-like processes have been recapitulated with ADTC5 cells (and engineered MSCs) previously, they require the use of long culture times and carefully controlled differentiation induction via chemicals (e.g., insulin, ascorbate, transferrin, etc.) or growth factors/cytokines (TGF-β, BMPs, PTHrP, IGF-1, etc.).[8,35,103,104]

The present behaviors/findings are fundamentally noteworthy in that neither growth factors, differentiation inducers, or substrate modification were used to regulate

chondrogenesis or neotissue formation, just chemogenetic activation of hM3Dq by CNO.

Although WT and unstimulated controls did not display evidence of extensive micro-tissue formation, cultures in which Ca^{2+} signaling was activated daily via TRPV4-mediated mechanisms occasionally exhibited ellipsoidal patches of increased cell density and modestly enhanced matrix staining at 14 days of culture. However, these cultures failed to generate the complex neotissues observed in CNO-simulated hM3Dq cultures.

Although nodule area/sizes were roughly the same under once-daily 5 nM CNO and once-daily 10 nM GSK101 stimulation, the CNO-evoked tissues displayed markedly more complex morphologies and alignments. We speculate that these differences could result from differences in cell tension and motility governed by hM3Dq versus activation; hM3Dq activation generated more extensive oscillatory signaling behaviors than TRPV4 activation,[40] and oscillatory calcium signaling has been shown to control cytoskeletal dynamics and cell motility in MSCs/chondroprogenitors.[2,105–107]

Indeed, we have observed that hM3Dq-ATDC5 cells appear to exhibit oscillatory changes in geometry suggestive of actomyosin-mediated contraction, and coincident with Ca^{2+} signals (unpublished observation). Based on these behaviors, one might postulate that induction of oscillatory $[Ca^{2+}]_i$ signaling in MSCs and pre-chondrocytes might serve to regulate cellular tractions and migrations, which are known to control/drive the formation of mesenchymal condensations that are necessary for chondrocyte differentiation.[108–112] Further, as these cells remodel their microenvironment/ECM, their calcium signaling dynamics may change, as was observed here.

The present work has leveraged the chemogenetic DREADD, hM3Dq, to establish a novel foundation from which the influence of $G\alpha_q$ signaling on chondrocyte physiology can be explored. However, the present approaches are not without their limitations. First, ATDC5 cells are an immortalized chondroprogenitor line; studies will be necessary to establish the efficacy of DREADD-mediated activation of Ca^{2+} signals on primary chondrocyte/MSC cell physiology.

Second, we only assessed hM3Dq-mediated outcomes in 2D culture; three-dimensional cultures, for which studies are ongoing, should provide more developmentally and contextually relevant testing environments to dissect the influence of hM3Dq-mediated $G\alpha_q$-GPCR activation on chondrocyte physiology *in situ.*

Third, although the neotissues formed here had many hallmarks of cartilage, more detailed studies are required to determine the precise composition of the elaborated matrix (i.e., hyaline cartilage vs. fibrocartilage) and their resultant gene expression/proteomic profiles. Lastly, a limited number of studies have shown the importance of $G\alpha_s$-coupled and $G\alpha_q$-coupled signaling in chondrocytes.[59,90] Although the present study focused solely on $G\alpha_q$-coupled signaling, $G\alpha_i$ and $G\alpha_s$-DREADDs are available for similar studies.[62]

Nonetheless, the hM3Dq DREADD system reported here represents a unique platform for directly interrogating the influence of $G\alpha_q$- and $[Ca^{2+}]_i$-signaling on chondrocyte physiology and cartilage health and pathology. Further, the synthetic activation of $G\alpha_q$-mediated signaling, through hM3Dq, represents a novel tool to direct toward improving cartilage tissue engineering and regeneration.

This study suggests that hM3Dq might be employed in place of, or alongside, traditional tissue engineering strategies to enhance, possibly in a synergistic manner, cartilage development/engineering *in vitro*. In addition, because $G\alpha_q$-linked chondrocyte outcomes are driven by the administration of an inexpensive, *inert,* small-molecule drug, there may be numerous benefits for studies targeted at improving cartilage engineering and regeneration using hM3Dq; namely, reductions in study costs (e.g., less reliance on chondrogenic growth factors) and complexity (e.g., reduced need for damaging physical perturbations of cells/tissue), its facile use in mixed/co-culture studies, and lastly, the unique potential for chemogenetically controlling hM3Dq-cells *in vivo* after implantation, in a manner that limits/eliminates non-target tissue effects.

Conclusion

Through the novel use of the chemogenetic DREADD, hM3Dq, within chondrocyte-like cells, we have generated several insights regarding the influence of targeted $G\alpha_q$-GPCR activation on (pre)chondrocyte physiology, and have further cemented the importance of $[Ca^{2+}]_i$ signaling and Ca^{2+} oscillations on both chondrogenesis and cartilage development. Together, the behaviors observed within synthetically activated hM3Dq-ATDC5 cells suggest that sustained, daily $G\alpha_q$ signaling can accelerate ATDC5 cell proliferation; a finding of benefit to exploring novel means to enhance chondrocyte precursor expansion *in vitro*.

Subsequently, daily $G\alpha_q$ activation appears to enhance neo-cartilage tissue formation, in a manner reminiscent of the mesenchymal condensation process that underpins long-bone patterning, endochondral ossification, and articular cartilage development, without the previous requirement of ''classical'' differentiation inducers. Ultimately, the present work has revealed a novel approach, namely chemogenetics, with which to precisely dissect the involvement of GPCR and Ca^{2+} signaling pathways in chondrocyte differentiation and homeostasis, and cartilage development and engineering.

Authors' Contributions

R.C.M.: contributed to the conception and design of the work, sole contributor to the acquisition of data, contributed to the analysis and interpretation of data, and drafted and revised the work. C.P.: contributed to the conception and design of the work, contributed to the analysis and interpretation of data, drafted and revised the work, and provided final approval of the version to be published.

Disclosure Statement

No competing financial interests exist.

Funding Information

This research was supported by a grant from NIH-NIGMS COBRE (P20 GM139760).

Supplementary Material

Supplementary Figure S1
Supplementary Figure S2
Supplementary Figure S3
Supplementary Figure S4
Supplementary Figure S5
Supplementary Figure S6
Supplementary Figure S7

References

1. Clapham, D.E. Calcium signaling. Cell **131,** 1047, 2007.
2. Matta, C., and Zakany, R. Calcium signalling in chondrogenesis: implications for cartilage repair. Front Biosci (Schol Ed) **5,** 305, 2013.
3. Sanchez, J.C., Danks, T.A., and Wilkins, R.J. Mechanisms involved in the increase in intracellular calcium following hypotonic shock in bovine articular chondrocytes. Gen Physiol Biophys **22,** 487, 2003.
4. Guilak, F., Zell, R., Erickson, G., and Grande, D. Mechanically induced calcium waves in articular chondrocytes are inhibited by gadolinium and amiloride. J Orthop Res **17,** 421, 1999.
5. Pingguan-Murphy, B., El-Azzeh, M., Bader, D.L., and Knight, M.M. Cyclic compression of chondrocytes modulates a purinergic calcium signalling pathway in a strain rate- and frequency-dependent manner. J Cell Physiol **209,** 389, 2006.
6. Edlich, M., Yellowley, C.E., Jacobs, C.R., and Donahue, H.J. Oscillating fluid flow regulates cytosolic calcium concentration in bovine articular chondrocytes. J Biomech **34,** 59, 2001.
7. Berridge, M.J., Bootman, M.D., and Roderick, H.L. Calcium signalling: dynamics, homeostasis and remodelling. Nat Rev Mol Cell Biol **4,** 517, 2003.
8. Trompeter, N., Gardinier, J., DeBarros, V., *et al.* Insulin-like Growth Factor-1 regulates the mechanosensitivity of chondrocytes by modulating TRPV4. bioRxiv **1950,** 1, 2020.
9. Horwitz, E.R., Higgins, T.M., and Harvey, B.J. Histamine-induced cytosolic calcium increase in porcine articular chondrocytes. Biochim Biophys Acta Mol Cell Res **1313,** 95, 1996.
10. Elfervig, M.K., Graff, R.D., Lee, G.M., Kelley, S.S., Sood, A., and Banes, A.J. ATP induces Ca2+ signaling in human chondrons cultured in three-dimensional agarose films. Osteoarthr Cartil **9,** 518, 2001.
11. Parekh, R., and Clark, A. Transforming growth factor-β elicits a calcium response in chondrocytes ex vivo. Osteoarthr Cartil **21,** S134, 2013.
12. Gilchrist, C.L., Leddy, H.A., Kaye, L., *et al.* TRPV4-mediated calcium signaling in mesenchymal stem cells regulates aligned collagen matrix formation and vinculin tension. Proc Natl Acad Sci U S A **116,** 1992, 2019.
13. San Antonio, J.D., and Tuan, R.S. Chondrogenesis of limb bud mesenchyme in vitro: stimulation by cations. Dev Biol **115,** 313, 1986.
14. Tomita, M., Reinhold, M.I., Molkentin, J.D., and Naski, M.C. Calcineurin and NFAT4 induce chondrogenesis. J Biol Chem **277,** 42214, 2002.
15. Steward, A.J. The role of calcium signalling in the chondrogenic response of mesenchymal stem cells to hydrostatic pressure. Eur Cells Mater **28,** 358, 2014.
16. Jacenko, O., and Tuan, R.S. Chondrogenic potential of chick embryonic calvaria: I. Low calcium permits cartilage differentiation. Dev Dyn **202,** 13, 1995.
17. Gavenis, K., Schumacher, C., Schneider, U., Eisfeld, J., Mollenhauer, J., and Schmidt-Rohlfing, B. Expression of ion channels of the TRP family in articular chondrocytes from osteoarthritic patients: changes between native and in vitro propagated chondrocytes. Mol Cell Biochem **321,** 135, 2009.
18. Huser, C.A.M., and Davies, M.E. Calcium signaling leads to mitochondrial depolarization in impact-induced chondrocyte death in equine articular cartilage explants. Arthritis Rheum **56,** 2322, 2007.
19. La Rovere, R.M.L., Roest, G., Bultynck, G., and Parys, J.B. Intracellular Ca2+ signaling and Ca2+ microdomains in the control of cell survival, apoptosis and autophagy. Cell Calcium **60,** 74, 2016.
20. Fewtrell, C. Ca2+ oscillations in non-excitable cells. Annu Rev Physiol **55,** 427, 1993.
21. Raizman, I., De Croos, J.N.A., Pilliar, R., and Kandel, R.A. Calcium regulates cyclic compression-induced early changes in chondrocytes during in vitro cartilage tissue formation. Cell Calcium **48,** 232, 2010.
22. Fitzgerald, J.B., Jin, M., Dean, D., Wood, D.J., Zheng, M.H., and Grodzinsky, A.J. Mechanical compression of cartilage explants induces multiple time-dependent gene expression patterns and involves intracellular calcium and cyclic AMP. J Biol Chem **279,** 19502, 2004.
23. Ye, B. Ca2+ oscillations and its transporters in mesenchymal stem cells. Physiol Res **59,** 323, 2010.
24. Gong, X., Xie, W., Wang, B., *et al.* Altered spontaneous calcium signaling of in situ chondrocytes in human osteoarthritic cartilage. Sci Rep **7,** 1, 2017.
25. Zhou, Y., Lv, M., Li, T., *et al.* Spontaneous calcium signaling of cartilage cells: from spatiotemporal features to biophysical modeling. FASEB J **33,** 4675, 2019.
26. Lv, M., Zhou, Y., Chen, X., Han, L., Wang, L., and Lu, X.L. Calcium signaling of in situ chondrocytes in articular cartilage under compressive loading: roles of calcium sources and cell membrane ion channels. J Orthop Res **36,** 730, 2017.
27. Zhou, Y., Park, M., Cheung, E., Wang, L., and Lu, X.L. The effect of chemically defined medium on spontaneous calcium signaling of in situ chondrocytes during long-term culture. J Biomech **48,** 990, 2015.
28. Weber, J.F., and Waldman, S.D. Calcium signaling as a novel method to optimize the biosynthetic response of chondrocytes to dynamic mechanical loading. Biomech Model Mechanobiol **13,** 1387, 2014.
29. Tomida, T., Hirose, K., Takizawa, A., Shibasaki, F., and Iino, M. NFAT functions as a working memory of Ca2+ signals in decoding Ca2+ oscillation. EMBO J **22,** 3825, 2003.
30. Dolmetsch, R.E., Xu, K., and Lewis, R.S. Calcium oscillations increase the efficiency and specificity of gene expression. Nature **392,** 933, 1998.
31. Hogan, P.G., Chen, L., Nardone, J., and Rao, A. Transcriptional regulation by calcium, calcineurin, and NFAT. Genes Dev **17,** 2205, 2003.
32. Argentaro, A., Sim, H., Kelly, S., *et al.* A SOX9 defect of calmodulin- dependent nuclear import in campomelic dysplasia/autosomal sex reversal. J Biol Chem **278,** 33839, 2003.
33. Uzieliene, I., Bernotas, P., Mobasheri, A., and Bernotiene, E. The role of physical stimuli on calcium channels in chondrogenic differentiation of mesenchymal stem cells. Int J Mol Sci **19,** 2998, 2018.

34. Mardani, M., Roshankhah, S., Hashemibeni, B., Salahshoor, M., Naghsh, E., and Esfandiari, E. Induction of chondrogenic differentiation of human adipose-derived stem cells by low frequency electric field. Adv Biomed Res **30,** 97, 2016.
35. Kwon, H.J., Lee, G.S., and Chun, H. Electrical stimulation drives chondrogenesis of mesenchymal stem cells in the absence of exogenous growth factors. Sci Rep **6,** 1, 2016.
36. Lin, S.-S., Tzeng, B.-H., Lee, K.-R., Smith, R.J.H., Campbell, K.P., and Chen, C.-C. Cav3.2 T-type calcium channel is required for the NFAT-dependent Sox9 expression in tracheal cartilage. Proc Natl Acad Sci U S A **111,** E1990, 2014.
37. Huang, C.-Y.C., Hagar, K.L., Frost, L.E., Sun, Y., and Cheung, H.S. Effects of cyclic compressive loading on chondrogenesis of rabbit bone-marrow derived mesenchymal stem cells. Stem Cells **22,** 313, 2004.
38. Steward, A.J., and Kelly, D.J. Mechanical regulation of mesenchymal stem cell differentiation. J Anat **227,** 717, 2015.
39. Kawano, S., Shoji, S., Ichinose, S., Yamagata, K., Tagami, M., and Hiraoka, M. Characterization of Ca2+ signaling pathways in human mesenchymal stem cells. Cell Calcium **32,** 165, 2002.
40. McDonough, R.C., Gilbert, R., Gleghorn, J., and Price, C. Targeted Gq-GPCR activation drives ER-dependent calcium oscillations in chondrocytes. Cell Calcium **94,** 1, 2021.
41. Matta, C., and Mobasheri, A. Regulation of chondrogenesis by protein kinase C: emerging new roles in calcium signalling. Cell Signal **26,** 979, 2014.
42. Bootman, M.D. Calcium signaling. Cold Spring Harb Perspect Biol **4,** 1, 2012.
43. Kawano, S., Otsu, K., Kuruma, A., *et al.* ATP autocrine/paracrine signaling induces calcium oscillations and NFAT activation in human mesenchymal stem cells. Cell Calcium **39,** 313, 2006.
44. VArga, Z., Juhasz, T., Matta, C., and Fodor, J. Switch of Voltage-Gated K+ channel expression in the plasma membrane of chondrogenic cells affects cytosolic Ca2+-oscillations and cartilage formation. PLoS One **6,** 27957, 2011.
45. O'Conor, C.J., Leddy, H.A., Benefield, H.C., Liedtke, W.B., and Guilak, F. TRPV4-mediated mechanotransduction regulates the metabolic response of chondrocytes to dynamic loading. Proc Natl Acad Sci U S A **111,** 1316, 2014.
46. McNulty, A.L., Leddy, H.A., Liedtke, W., and Guilak, F. TRPV4 as a therapeutic target for joint diseases. Naunyn Schmiedebergs Arch Pharmacol **388,** 437, 2015.
47. Hanna, H., Andre, F.M., and Mir, L.M. Electrical control of calcium oscillations in mesenchymal stem cells using microsecond pulsed electric fields. Stem Cell Res Ther **8,** 91, 2017.
48. Vincent, F., Acevedo, A., Nguyen, M.T., *et al.* Identification and characterization of novel TRPV4 modulators. Biochem Biophys Res Commun **389,** 490, 2009.
49. Mobasheri, A., and Martín-Vasallo, P. Epithelial sodium channels in skeletal cells; A role in mechanotransduction? Cell Biol Int **23,** 237, 1999.
50. Nagao, M., Ishii, S., and Yabu, H. Voltage-gated ionic channels in cultured rabbit articular chondrocytes. Comp Biochem Physiol Part C Pharmacol Toxicol Endocrinol **115,** 223, 1996.
51. Vriens, J., Appendino, G., and Nilius, B. Pharmacology of vanilloid transient receptor potential cation channels. Mol Pharmacol **75,** 1262, 2009.
52. Rojas, A., Padidam, M., Cress, D., and Grady, W.M. TGF-beta receptor levels regulate the specificity of signaling pathway activation and biological effects of TGF-beta. Biochim Biophys Acta **1793,** 1165, 2009.
53. McDonough, R.C., Shoga, J.S., and Price, C. DREADD-based synthetic control of chondrocyte calcium signaling in vitro. J Orthop Res **37,** 1518, 2019.
54. Armbruster, B.N., Li, X., Pausch, M.H., Herlitze, S., and Roth, B.L. Evolving the lock to fit the key to create a family of G protein-coupled receptors potently activated by an inert ligand. Proc Natl Acad Sci U S A **104,** 5163, 2007.
55. Prosser, R.S., and Kim, T.H. G Protein-coupled receptors in drug discovery. Methods Mol Biol **1335,** 39, 2015.
56. Tuteja, N. Signaling through G protein coupled receptors. Plant Signal Behav **4,** 942, 2009.
57. Leurs, R., Bakker, R.A., Timmerman, H., and de Esch, I.J.P. The histamine H3 receptor: from gene cloning to H3 receptor drugs. Nat Rev Drug Discov **4,** 107, 2005.
58. Li, J., Ning, Y., Hedley, W., *et al.* The molecule pages database. Nature **420,** 716, 2002.
59. Chagin, A.S., Vuppalapati, K.K., Kobayashi, T., *et al.* G-protein stimulatory subunit alpha and Gq/11alpha G-proteins are both required to maintain quiescent stem-like chondrocytes. Nat Commun **5,** 3673, 2014.
60. Smith, K.S., Bucci, D.J., Luikart, B.W., and Mahler, S.V. DREADDS: use and application in behavioral neuroscience. Behav Neurosci **130,** 137, 2016.
61. Zhu, H., and Roth, B.L. DREADD: a chemogenetic GPCR signaling platform. Int J Neuropsychopharmacol **18,** pyu007, 2014.
62. Rogan, S.C., and Roth, B.L. Remote control of neuronal signaling. Pharmacol Rev **63,** 291, 2011.
63. Barrett-Jolley, R., Lewis, R., Fallman, R., and Mobasheri, A. The emerging chondrocyte channelome. Front Physiol **1,** 1, 2010.
64. Grundmann, M., and Kostenis, E. Temporal bias: time-encoded dynamic GPCR signaling the temporal dimension of g-protein-coupled receptor signaling. TRENDS Pharmacol Sci **38,** 1110, 2017.
65. Alexander, G.M., Rogan, S.C., Abbas, A.I., *et al.* Remote control of neuronal activity in transgenic mice expressing evolved G protein-coupled receptors. Neuron **63,** 27, 2009.
66. Krashes, M.J., Koda, S., Ye, C., *et al.* Rapid, reversible activation of AgRP neurons drives feeding behavior in mice. J Clin Invest **121,** 1424, 2011.
67. Jain, S., De Azua, I.R., Lu, H., White, M.F., Guettier, J.M., and Wess, J. Chronic activation of a designer Gq-coupled receptor improves β cell function. J Clin Invest **123,** 1750, 2013.
68. Hua Li, J., Jain, S., McMillin, S.M., *et al.* A novel experimental strategy to assess the metabolic effects of selective activation of a g q - coupled receptor in hepatocytes in vivo. Endocrinology **154,** 3539, 2013.
69. Kaufmann, A., Keim, A., and Thiel, G. Regulation of immediate-early gene transcription following activation of Gq-coupled designer receptors. J Cell Biochem **114,** 681, 2013.
70. David, M.A., Smith, M.K., Pilachowski, R.N., White, A.T., Locke, R.C., and Price, C. Early, focal changes in cartilage cellularity and structure following surgically

induced meniscal destabilization in the mouse. J Orthop Res **35,** 537, 2017.
71. Rousseeuw, P.J., and Hubert, M. Robust statistics for outlier detection. Wiley Interdiscip Rev Data Min Knowl Discov **1,** 73, 2011.
72. Fitzgerald, J.B., Jin, M., and Grodzinsky, A.J. Shear and compression differentially regulate clusters of functionally related temporal transcription patterns in cartilage tissue. J Biol Chem **281,** 24095, 2006.
73. Waldman, S.D., Couto, D.C., Grynpas, M.D., Pilliar, R.M., and Kandel, R.A. A single application of cyclic loading can accelerate matrix deposition and enhance the properties of tissue-engineered cartilage. Osteoarthr Cartil **14,** 323, 2006.
74. Parate, Di, Franco-Obregón, A., Fröhlich, J., *et al.* Enhancement of mesenchymal stem cell chondrogenesis with short-term low intensity pulsed electromagnetic fields. Sci Rep **7,** 1, 2017.
75. Newton, P.T., Staines, K.A., Spevak, L., *et al.* Chondrogenic ATDC5 cells: an optimised model for rapid and physiological matrix mineralisation. Int J Mol Med **30,** 1187, 2012.
76. Shukunami, C., Shigeno, C., Atsumi, T., Ishizeki, K., Suzuki, F., and Hiraki, Y. Chondrogenic Differentiation of Clonal Mouse Embryonic Cell Line ATDC5 In Vitro: differentiation-dependent Gene Expression of Parathyroid Hormone (PTH)/PTH-related Peptide Receptor. J Cell Biol **133,** 457, 1996.
77. Yao, Y., Zeng, L., and Huang, Y. The enhancement of chondrogenesis of ATDC5 cells in RGD-immobilized microcavitary alginate hydrogels. Hard Tissues Mater **31,** 92, 2016.
78. Atsumi', T., Miwa, Y., Kimata, K., and Ikawa, Y. A chondrogenic cell line derived from a differentiating culture of AT805 teratocarcinoma cells. Cell Differ Dev **30,** 109, 1990.
79. Yang, D., Song, L.S., Zhu, W.Z., *et al.* Calmodulin regulation of excitation-contraction coupling in cardiac myocytes. Circ Res **92,** 659, 2003.
80. Yáñez, M., Gil-Longo, J., and Campos-Toimil, M. Calcium binding proteins. Adv Exp Med Biol **740,** 461, 2012.
81. Kordowska, J., Huang, R., and Wang, C.L.A. Phosphorylation of caldesmon during smooth muscle contraction and cell migration or proliferation. J Biomed Sci **13,** 159, 2006.
82. Hamilton, S.L., Serysheva, I., and Strasburg, G.M. Calmodulin and excitation-contraction coupling. J Physiol **15,** 281, 2000.
83. Elíes, J., Yáñez, M., Pereira, T.M.C., Gil-Longo, J., MacDougall, D.A., and Campos-Toimil, M. An update to calcium binding proteins. Adv Exp Med Biol **1131,** 183, 2020.
84. Zhang, W., and Gunst, S.J. Non-muscle (NM) myosin heavy chain phosphorylation regulates the formation of NM myosin filaments, adhesome assembly and smooth muscle contraction. J Physiol **595,** 4279, 2017.
85. Winder, S.J., and Walsh, M.P. Calponin: thin filament-linked regulation of smooth muscle contraction. Cell Signal **5,** 677, 1993.
86. Lembong, J., Sabass, B., and Stone, H.A. Calcium oscillations in wounded fibroblast monolayers are spatially regulated through substrate mechanics. Phys Biol **14,** 1, 2017.
87. Kim, T.J., Seong, J., Ouyang, M., *et al.* Substrate rigidity regulates Ca2+ oscillation via RhoA pathway in stem cells. J Cell Physiol **218,** 285, 2009.
88. Sun, S., Liu, Y., Lipsky, S., and Cho, M. Physical manipulation of calcium oscillations facilitates osteodifferentiation of human mesenchymal stem cells. FASEB J **21,** 1472, 2007.
89. Nurminsky, D., Magee, C., Faverman, L., and Nurminskaya, M. Regulation of chondrocyte differentiation by actin-severing protein adseverin. Dev Biol **302,** 427, 2007.
90. Chagin, A.S., and Kronenberg, H.M. Role of G-proteins in the differentiation of epiphyseal chondrocytes. J Mol Endocrinol **53,** R39, 2014.
91. Blanco, F.J., López-Armada, M.J., and Maneiro, E. Mitochondrial dysfunction in osteoarthritis. Mitochondrion **4,** 715, 2004.
92. Amin, A.K., Huntley, J.S., Bush, P.G., Simpson, A.H.R.W., and Hall, A.C. Chondrocyte death in mechanically injured articular cartilage-the influence of extracellular calcium. J Orthop Res **27,** 778, 2009.
93. Sanchez-Adams, J., Leddy, H.A., McNulty, A.L., O'Conor, C.J., and Guilak, F. The mechanobiology of articular cartilage: bearing the Burden of Osteoarthritis. Curr Rheumatol Rep **16,** 1, 2014.
94. Loukin, S., Su, Z., and Kung, C. Increased basal activity is a key determinant in the severity of human skeletal dysplasia caused by TRPV4 mutations. PLoS One **6,** 1, 2011.
95. Thompson, M.D., Burnham, W.M.I., and Cole, D.E.C. The G protein-coupled receptors: pharmacogenetics and disease. Crit Rev Clin Lab Sci **42,** 311, 2005.
96. Jean-Alphonse, F., and Hanyaloglu, A.C. Regulation of GPCR signal networks via membrane trafficking. Mol Cell Endocrinol **331,** 205, 2011.
97. Goldring, M.B. Chondrogenesis, chondrocyte differentiation, and articular cartilage metabolism in health and osteoarthritis. Ther Adv Musculoskelet Dis **4,** 269, 2012.
98. Hall, B.K., and Miyake, T. All for one and one for all: condensations and the initiation of skeletal development. BioEssays **22,** 138, 2000.
99. Yang, Y., Liu, Y., Lin, Z., *et al.* Condensation-driven chondrogenesis of human mesenchymal stem cells within their own extracellular matrix: formation of cartilage with low hypertrophy and physiologically relevant mechanical properties. Adv Biosyst **3,** 1900229, 2019.
100. Klumpers, D.D., Mao, A.S., Smit, T.H., and Mooney, D.J. Linear patterning of mesenchymal condensations is modulated by geometric constraints. J R Soc Interface **11,** 95, 2014.
101. McDermott, A.M., Herberg, S., Mason, D.E., *et al.* Recapitulating bone development through engineered mesenchymal condensations and mechanical cues for tissue regeneration. Sci Transl Med **11,** 7756, 2019.
102. Ghosh, S., Laha, M., Mondal, S., Sengupta, S., and Kaplan, D.L. In vitro model of mesenchymal condensation during chondrogenic development. Biomaterials **30,** 6530, 2009.
103. Weiss, H.E., Roberts, S.J., Schrooten, J., and Luyten, F.P. A semi-autonomous model of endochondral ossification for developmental tissue engineering. Tissue Eng Part A **18,** 1334, 2012.
104. Ray, P., and Chapman, S.C. Cytoskeletal reorganization drives mesenchymal condensation and regulates downstream molecular signaling. PLoS One **10,** e0134702, 2015.

105. Panadero, J.A., Lanceros-Mendez, S., and Ribelles, J.L.G. Differentiation of mesenchymal stem cells for cartilage tissue engineering: individual and synergetic effects of three-dimensional environment and mechanical loading. Acta Biomater **33,** 1, 2016.
106. Gardinier, J.D., Majumdar, S., Duncan, R.L., and Wang, L. Cyclic hydraulic pressure and fluid flow differentially modulate cytoskeleton re-organization in MC3T3 Osteoblasts. Cell Mol Bioeng **2,** 133, 2009.
107. Chao, P.-H.G., West, A.C., and Hung, C.T. Chondrocyte intracellular calcium, cytoskeletal organization, and gene expression responses to dynamic osmotic loading. Am J Physiol Cell Physiol **291,** C718, 2006.
108. Rodríguez, J.P., González, M., Ríos, S., and Cambiazo, V. Cytoskeletal organization of human mesenchymal stem cells (MSC) changes during their osteogenic differentiation. J Cell Biochem **93,** 721, 2004.
109. Heo, S.J., Han, W.M., Szczesny, S.E., *et al.* Mechanically induced chromatin condensation requires cellular contractility in mesenchymal stem cells. Biophys J **111,** 864, 2016.
110. Bouvard, D., and Block, M.R. Calcium/calmodulin-dependent protein kinase II controls integrin $\alpha 5\beta 1$-mediated cell adhesion through the integrin cytoplasmic domain associated protein-1α. Biochem Biophys Res Commun **181,** 1217, 1998.
111. Gershlak1, J.R., Resnikoff, J.I., Sullivan, K.E., Williams, C., Wang, R.M., and Black, III L.D. Mesenchymal stem cells ability to generate traction stress in response to substrate stiffness is modulated by the changing extracellular matrix composition of the heart during development. Bone **23,** 1, 2011.
112. Pchelintseva, E., and Djamgoz, M.B.A. Mesenchymal stem cell differentiation: control by calcium-activated potassium channels. J Cell Physiol **233,** 3755, 2018.

Address correspondence to:
Christopher Price, PhD
Department of Biomedical Engineering
University of Delaware
590 Avenue 1743
Newark, DE 19713
USA

E-mail: cprice@udel.edu

Received: April 2, 2021
Accepted: October 11, 2021
Online Publication Date: December 24, 2021